# Isotropic T2 Mapping using a 3D Radial FSE (or TSE) pulse sequence

Mahesh Bharath Keerthivasan[1], Ali Bilgin[1,2], Diego R Martin[2], and Maria I Altbach[2]
[1]*Electrical and Computer Engineering, University of Arizona, Tucson, Arizona, United States,* [2]*Medical Imaging, University of Arizona, Tucson, Arizona, United States*

**Introduction**: T2-weighted imaging and quantitative characterization of tissue based on T2 mapping plays an important role in the diagnosis of pathologies. Techniques based on spin-echo (SE) or fast spin-echo (FSE) sequences are time consuming because they require multiple acquisitions for obtaining an adequate number of TE images for accurate T2 mapping. Radial FSE based methods have been shown to generate accurate T2 maps from a single acquisition using highly undersampled data [1][2]. These techniques are limited to multi-slice 2D imaging. 3D imaging and 3D T2 mapping [3] are useful in applications where the anatomical structure can be better viewed by reformatting an isotropic voxel. Recently, a radial 3D FSE pulse sequence was presented [4] and it was shown to be less sensitive to motion compared to a Cartesian counterpart. In this work, we present a technique for isotropic T2 mapping that uses data collected using a radial 3D FSE pulse sequence and a reconstruction technique that generates T2 maps from highly undersampled data.

**Technique**: A commercial 3D FSE pulse sequence was modified to support a stack-of-stars radial trajectory. The sequence diagram for a non-selective 3D radial FSE sequence is shown in Figure 1. Each plane of k-space is collected using a radial trajectory with a bit-reversed view ordering that has been shown [5] to minimize artifacts from T2 decay. A T2 mapping technique with indirect echo compensation (CURLIE) [1] was extended to work with the 3D radial data. CURLIE is based in the Slice resolved Extended Phase Graph (SEPG) formulation [6] and thus, accounts for indirect echoes caused by non-180$^o$ refocusing pulses. Because the data acquired for each TE time point are highly under-sampled (only 4 radial lines per TE are acquired), CURLIE incorporates the SEPG model into a model based iterative reconstruction to estimate *T2* together with the equilibrium magnetization ($I_o$) and the *B1* field map for all voxels:

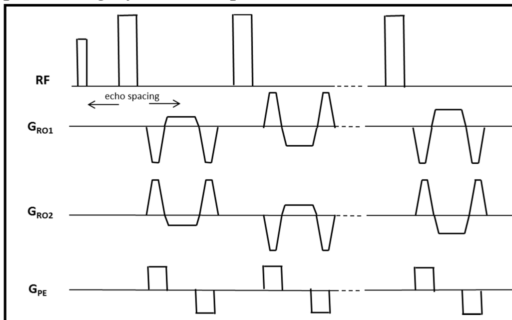


Figure 1: Diagram of a 3D Radial FSE sequence

$$argmin_{I_0,T2,B1} \sum_{j=1}^{n} \left|\left| FT\{C_j(I_0, T2, B1, \alpha_0, \ldots, \alpha_j)\} - K_j \right|\right|_2^2 \quad (1).$$

In (1) *FT* is the forward Fourier Transform, $K_j$ is the undersampled k-space data at the $j^{th}$ TE, and $C_j$ is the SEPG model expressed as a function of $I_0$, *T2*, *B1* and the flip angles of the excitation and refocusing RF pulses. CURLIE uses a principal component approach to linearize the non-linear SEPG signal model. For the desired range of *T2* and *B1* values, decay curves are generated and used as a training set to generate the principal components. The vector representing the *T2* decay curve with indirect echoes $\vec{v}$ can be approximated as a weighted linear combination of these principal components, with weight $m_i$ for the i$^{th}$ principal component $\vec{p_i}$ , $\vec{v} = \sum_{i=1}^{L} m_i \vec{p_i}$ . Writing $\vec{M_i}$ as the vector of $m_i$ for all the voxels the matrix $M$ can be formed as $(\vec{M_1}, \vec{M_2}, \ldots, \vec{M_L})$ and the matrix of the first $L$ principal components can be written as $P = (\vec{P_1}, \vec{P_2}, \ldots, \vec{P_L})$ . The image at $TE_j$ can now be obtained using just the L principal component coefficients as $M\, P_j^T$ where $P_j$ is the j$^{th}$ row of the matrix $P$. The linearized formulation of the reconstruction algorithm is now given by:

$$argmin_M \sum_{l=1}^{coils} \sum_{j=1}^{n} \left|\left| FT_j(S_l M P_j^T) - K_{l,j} \right|\right|_2^2 + \lambda\, ||\psi M||_1 \quad (2).$$

Here $S_l$ corresponds to the complex coil sensitivities and the penalty terms are used to exploit the spatial compressibility of the principal component coefficient maps using a sparsity transform $\psi$. The above linear problem is solved using a conjugate gradient based minimization approach and the TE images are reconstructed from *M*. The *T2* maps are then estimated by fitting the TE decay curves per voxel using the SEPG model.

**Methods**: The sequence was tested on a 3T Siemens scanner. A set of gel phantoms with different T2 times were prepared and used to acquire data using the Radial 3D FSE sequence with ETL=64, matrix size=256x256, TR=1600ms and echo spacing=7.1ms. Reference data were acquired using a Cartesian 2D SE pulse sequence because the method is not affected by indirect echoes. SE data were acquired with matrix size = 256x256, TR = 1500ms, and it was repeated for different TE values in increments of 7ms. In vivo brain data were acquired with 1.2 mm isotropic resolution, ETL=64, TR=1600 ms and echo spacing=7.1ms. The range of T2 values used for principal component training was 30 – 500ms.

**Table 1: Mean T2 values (ms)**

| Phantom | 2D SE (reference) | 3D Radial TSE |
|---|---|---|
| 1 | 68.38 ± 2.54 | 66.76 ± 4.62 |
| 2 | 134.52 ± 5.39 | 138.43 ± 3.21 |
| 3 | 140.77 ± 6.37 | 143.12 ± 8.38 |
| 4 | 113.65 ± 3.04 | 117.21 ± 5.42 |

**Results:** Table 1 shows the estimated mean T2 values and standard deviation for four different phantoms for the 3D T2 mapping technique along with those obtained from the reference SE sequence. Note that the mean T2 values from the 3D FSE fall within the same range as the values obtained from the SE measurements. Figure 2 shows the coronal, sagittal and axial cross sections of the anatomical brain image acquired using the radial 3D FSE sequence. The T2 maps corresponding to the same slices are shown in Figure 3.

**Conclusion**: An isotropic T2 mapping technique based on a 3D FSE sequence has been presented. The results show that the T2 maps from the 3D TSE sequence are comparable to those from a traditional SE experiment. The technique has the advantage of providing high resolution T2 maps in any desired cross section.

**References:** [1] Huang MRM 70(4) 2013 [2] Altbach MRM 54 2005 [3] Staroswiecki MRM 67(4) 2012 [4] Mugler 2013 Proc. ISMRM 2013 [5] Theilmann MRM 51(4) 2004 [6] Lebel MRM 64 2010

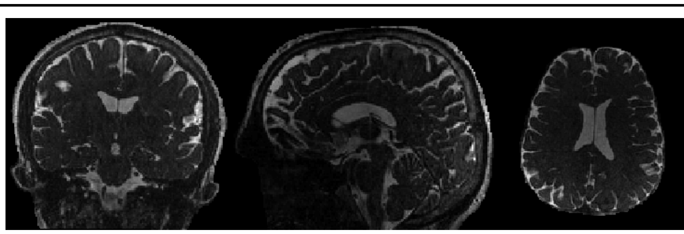

Figure 2: Coronal, Sagittal and Axial images from the radial 3D TSE sequence

Figure 3: T2 map of the brain for the three cross sections